A&A 410, 269–282 (2003)
DOI: 10.1051/0004-6361:20031242

Astronomy & Astrophysics

The short period multiplicity among T Tauri stars⋆

C. H. F. Melo⋆⋆

European Southern Observatory, Casilla 19001, Santiago 19, Chile
Observatoire de Genève, Ch. des Maillettes 51, 1290 Sauverny, Switzerland

Received 11 December 2002 / Accepted 30 July 2003

Abstract. We present the results of high-resolution spectroscopic observations carried out over three years aimed at estimating the short-period ($P_{\rm orb}$ < 100 days) binary frequency of a sample of T Tauri stars in Oph-Sco, Cha, Lup, CrA star forming regions (SFRs), already observed with high angular resolution techniques by Ghez et al. (1993) and by Ghez et al. (1997) to detect wider components. When combining all four SFRs, the short-period binary frequency is indistinguishable from that found by Duquennoy & Mayor (1991) for the solar-type field stars which is also consistent with the previous result obtained by Mathieu (1992, 1994). When Oph-Sco is analyzed separately, it seems that there is an excess of short-period binaries of a factor 2–2.5. On the contrary, short-period binary systems seem to be absent in the sample containing stars in Cha/Lup/CrA. Such a trend was equally found by Mathieu (1992) in Taurus. An excess of spectroscopic systems among the components of visual multiple systems is also observed.

Key words. stars: binaries: close – stars: formation

1. Introduction

High-angular resolution techniques have been widely used in the last decade to measure the binary frequency among the low-mass pre-main sequence populations in the nearby star-forming regions (e.g. Ghez et al. 1993, 1997; Leinert et al. 1993; Richichi et al. 1994; Brandner & Köhler 1998) and among low-mass solar-type stars in young clusters (e.g., Bouvier et al. 1997; Patience et al. 1998; Duchêne et al. 1999; Patience & Duchêne 2001 and references therein).

The results of these surveys qualitatively suggest that the binary frequency is indeed larger among pre-main sequence (PMS) stars than among the solar–type stars (Duquennoy & Mayor 1991). However, a direct comparison of the results is somewhat difficult due to differences in the sample size and detection limits of each survey.

Duchêne (1999) partially solves the issue by applying a correction for missed companions (when required) and by normalizing the results of individual surveys by the analytical expression for the binary frequency among G- and K-dwarfs of the solar neighborhood given by Duquennoy & Mayor (1991) in the corresponding interval of separation. If it is further assumed that all distributions of binary frequency as a function of separation between the components or orbital period are Gaussians and that they peak at the same place as for the main-sequence (MS) G and K-dwarfs, then the procedure of Duchêne (1999) can be used to answer the question of whether the binary frequency is higher among the young objects as suggested by the results of these first surveys. In this case, the overall binary frequency is just an extrapolation of the limited binary frequency derived by a small range of orbital period. Patience & Duchêne (2001) analyzed these normalized companion star fractions (CSFs) and concluded that they are better correlated with the density of the SFR/cluster than with age which could indicate that the binary frequency of a given population is set by the physical conditions of its parental cloud.

If, however, these two assumptions are incorrect then the whole binary frequency distribution as a function of orbital period must be known in order to assess the overall binary frequency. Indeed, the results of Brandner & Köhler (1998) support the non-validity of these two assumptions. They carried out *K*-band speckle observations in two sub-regions of Scorpious-Centaurus OB association, namely, Upper-Scorpious A and B. In the Upper-Sco A, T Tauri stars are associated with B-type stars whereas in Upper-Sco B, only a few early-type stars are present. Their results give a similar binary frequency for both sub-regions (about 31% ± 7% for US-A and 39% ± 9% for US-B), nevertheless the closer binaries are much more numerous in US-A than in US-B. Their conclusion is that the same physical conditions that facilitate the formation of massive stars also help in the formation of closer binaries among low-mass stars.

Thus, to discern whether there exists a real overall excess and a difference in the shape of the binary frequency distribution, we must first determine the PMS binary frequency distribution for a large range of orbital period as previously done by Duquennoy & Mayor (1991) for MS stars. Their sample however is defined inside a sphere of about 20 pc, while for the PMS case the closest star-forming regions are about 150 pc away. This fact added to the present sensitivity of high-angular resolution experiments limits the determination of the PMS binary frequency distribution to a narrow strip of orbital period

⋆ Based on observations collected with the Swiss Euler Telescope and 1.5-m ESO, proposal 63.I-0112.

⋆⋆ e-mail: cmelo@eso.org

from $10^{3.5}$ to $10^{7.5}$ days. As a consequence, the comparison between MS and PMS binary frequency remains very poor.

Currently, the short-period part of the PMS binary frequency distrubution can only be assessed by spectroscopic observations. In order to determine it, we began in June 1998, a spectroscopic monitoring of the southern part of the sample of Ghez et al. (1993, hereafter GNM93), i.e., Oph-Sco stars, and entire sample of Ghez et al. (1997, hereafter GMPB97). The survey was carried out with the high-resolution spectrograph CORALIE (e.g. Queloz et al. 2000) mounted at the Euler Swiss Telescope and FEROS (Kauffer et al. 1999) mounted at the 1.5-m ESO Observatory, both at La Silla, Chile. In this paper we present the results of this campaign.

This paper is organized as follow. Section 2 presents the observations and data reduction. Section 3 presents radial velocity measurements with individual discussions of some relevant objects. Finally, we compute the companion star fraction for our sample and discuss the implications to the binary formation scenarios in Sect. 4.

2. Sample and spectroscopic observations

The main aim of this study is to search for close companions which could not be detected by the speckle studies of GNM93 and GMPR97. Thus, we chose the same sample as in GMPR97 and the southern sample of GMPR97, i.e., the Oph-Sco objects. In Table 1 we present our sample which consists of 88 stars. Several of these 88 stars (12 objects) were too faint to be observed with the Swiss Telescope. Some of them were observed with the ESO 1.5 m telescope. The sample studied in GMPR97 includes 3 Herbig Ae/Be stars which were not observed, as we were interested only on the T Tauri stars. Also, the 9 Weak-line T Tauri stars (WTTS or NTTS) (Walter et al. 1994) previously studied by Mathieu et al. (1989) were not observed either, since the potential spectroscopic companions have already been found. Thus, our final sample used to compute the short-period binary frequency counts 65 stars.

Most of the spectroscopic observations were carried out using the two-fiber-fed high-resolution spectrograph CORALIE ($\lambda/\Delta\lambda \sim 48\,000$) attached to the Swiss Euler Telescope. The CORALIE spectra were collected in three different seasons, namely, July 1998, May 1999 and Apr. 2000. All observations were taken in the OBJ2 mode, i.e., one fiber centered on the target star and the other fiber illuminated by the background sky. The sky fiber information was important to subtract an eventual contamination by moonlight. The reduction was performed by the CORALIE pipe-line reduction software which yields a fully reduced spectrum (extracted, flat-fielded and dispersion corrected) and the cross-correlation function (CCF) in a few minutes after the acquisition of the exposure. The CORALIE pipe-line software reduction is based on INTER-TACOS software (Queloz 1995).

A few observations were performed with the two-fiber-fed spectrograph FEROS ($\lambda/\Delta\lambda \sim 50\,000$) attached to the 1.5-m/ESO. They were collected in only one run in May 1999. Similar to CORALIE observations, these observations were equally taken in the OS (Object-Sky) mode and make use of a pipe-line data reduction which gives as the final product a 1D spectrum. For these spectra, the CCFs were computed off-line using the INTER-TACOS software.

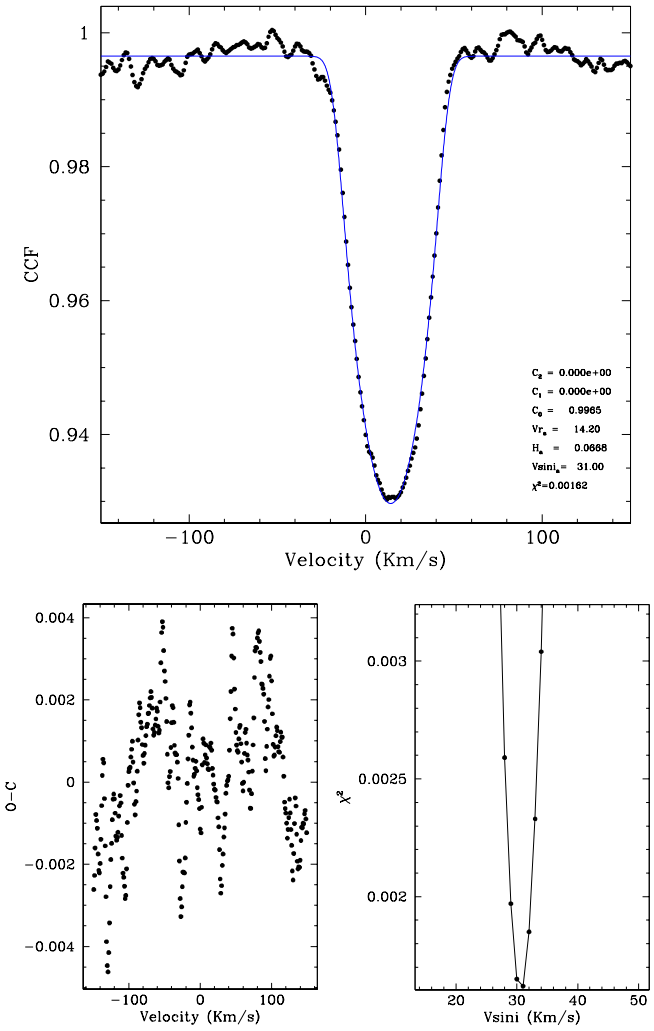

Fig. 1. An example of the fit procedure described in Sect. 2.1. *Top*. The CCF for Sz 41 a moderate rotator ($V \sin i = 31$ km s^{-1}). The bottom of the CCF is not very well fitted probably due to spots in the surface of star. *Bottom-left*. The residuals (O–C) of the fit. *Bottom-right*. The $\chi^2_{V \sin i}$ as a function of the $V \sin i$.

2.1. Radial velocity determination

Radial velocities were derived from the CCF which is computed by convolving the observed spectrum with a K0V CORAVEL-type numerical mask (Queloz 1995). For each observation, the CCF is fitted by a family of functions $CCF_{V \sin i} = C - D[g_0 \otimes G(V \sin i)]$ which is the result of the convolution of the CCF of a non-rotating star g_0, which can be fairly approximated by a Gaussian, and the Gray (1976) rotational profile computed for several rotational velocities $G(V \sin i)$. For each function $CCF_{V \sin i}$ we found the radial velocity V_r, the depth D and the continuum C for minimizing the quantity $\chi^2_{V \sin i}$ which is the traditional χ^2 function (e.g. Press et al. 1992, Eq. (15.1.5)) with $\sigma_i = 1$, where σ_i is the measurement error. Figure 1 shows an example of the fit procedure described.

Table 1. Sample studied in this work. Column 1: object identity according to that used in GNM93 and GMPR97; Col. 2: number of measurements per object; Col. 3: mean radial velocity (in km s^{-1}); Col. 4: rms of the radial velocity measurements (in km s^{-1}); Col. 5: visual multiplicty status (S-single star, B-binary star, T-Triple star); Cols. 6–7: the angular separation in arc-seconds ρ and the position angle PA of an eventual visual companion; Col. 8: reference for the values of Cols. 6–7; Col. 9: orbital period of an eventual spectroscopic companion; Col. 10: references for the values of Col. 9.

Name	N_{obs}	$\overline{V_r}$	σ_{V_r}	Type	Imaging/Speckle			Spectroscopy	
					ρ ($''$)	PA ($^\circ$)	Ref.	P_{orb} (days)	Ref.
Cha I									
SZ Cha[1]	7	16.10	0.78	B	5.3	121	GMPR97		
LHα 332-20	4	15.33	0.67	S					
CS Cha	6	15.73	1.07	S					
CT Cha	6	15.15	0.69	S					
Ced 110	...			S					
LHα 332-17	8	13.92	0.92	B	4.9	202	GMPR97		
HM 15	6	14.38	0.63	S					
Sz 22	...			S					
VW Cha	2	16.96	2.33	T	0.66	184	GMPR97	SB?	
					2.7	56			
HD 97048	...			S					
CHXR 32	6	10.67	1.17	B	2.5	284	GMPR97		
C9-2	...			S					
VZ Cha	2	17.97	1.12	S					
HD 97300	...			B	0.84	327	GMPR97		
Sz 32	...			S					
WW Cha	...			S					
WX Cha	...			B	0.79	55	GMPR97		
WY Cha	...			S					
C7-11	...			B	1.2	156	GMPR97		
CHX 18N	6	15.51	0.60	S			GMPR97	SB?	
Sz 41[1]	8	14.18	0.55	B	1.50	150	GMPR97		
LHα 332-21[1]	7	15.57	0.82	B	11.70	98	GMPR97		
HM Anon	6	14.04	0.17	B	0.27	236	GMPR97		
Cha II									
BF Cha	4	11.45	1.23	S				SB?	
BM Cha	1	10.30	2.50	S					
Lup I									
Sz 65	5	−0.82	1.49	B	6.50	97	GMPR97		
Sz 68	8	−2.31	0.60	T	0.107	245	GMPR97		
					2.8	296	GMPR97		
GW Lup	2	−2.46	1.75	S					
GQ Lup	6	−3.17	0.69	S					
HM Lup	...								
Sz 73	1	−3.28	2.50	S					
HN Lup	...			B	0.24	359	GMPR97		
Sz 77	6	−2.60	0.33	B	1.8	205	GMPR97		
Lup II									
Sz 78	6	−6.44	0.09	S					
Sz 79	7	−88.59	0.06	S					
Th 12	8	−0.86	0.70	S					
RU Lup	7	−0.94	1.18	S					
Lup IV									
RY Lup	7	−2.03	0.88	S					
He 1125	6	−0.14	0.61	S					
Sz 85	4	−25.19	1.29	S					
Sz 126	1	−0.64	2.50	S					
Sz 128	2	−0.80	1.28	S					
Sz 130	3	0.62	0.43	S					

[1] Unpublished CORAVEL data spanning from a Julian Date 47 500 up to 50 000 present a mean radial velocity similar to our mean measurements (Reipurt, private communication).

Table 1. continued.

Name	N_{obs}	$\overline{V_r}$	σ_{V_r}	Type	Imaging/Speckle			Spectroscopy	
					ρ ($''$)	PA ($^\circ$)	Ref.	P_{orb} (days)	Ref.
				Lup III					
EX Lup	2	−1.45	2.31	S					
Sz 89	2	−37.55	0.78	S					
HO Lup	3	−2.99	0.49	B	1.49	35	GMPR97		
Sz 90	5	0.21	2.20	S					
Sz 91	3	−1.57	0.97	B	8.7	120	GMPR97		
Sz 96	3	−3.49	0.20	S					
HK Lup	3	−1.88	2.14	S					
Sz 103	1	−1.32	2.50	S					
HR 5999	...			B	1.53	114	GMPR97		
Sz 105	1	1.70	2.50	B	10.9	320	GMPR97		
Sz 110	2	−0.25	0.74	S					
Sz 111	1	−1.35	2.50	S					
Sz 117	4	−1.75	1.23	S					
Sz 120	...			B	2.7	142	GMPR97		
Sz 123	2	−0.33	0.35	B	1.7	296	GMPR97		
				Cr A					
KnHα 6	3	−2.35	1.59	S					
S CrA	7	−0.30	1.74	B	1.41	157	GMPR97		
Wa CrA/1	...			S					
R CrA	...			S					
T CrA	...			S					
VV CrA	...			B	2.1	48	GMPR97		
				Sco-Oph					
AS 205	6	−9.38	1.51	B	1.32	212	GNM93	SB?	
DoAr 21	...			S					
RNO 90	...			S					
DoAr 24 E	1	−7.97	2.50	B	2.03	150	GNM93		
ROXs 43A	...			B	6.0	13	BA92	89.10	MWM89
V1121 Oph	6	−8.62	0.47	S					
SR 9	12	−7.11	1.30	B	0.59	350	GNM93		
SR 24 S	...			S					
NTTS 155203-2338	1	−3.94	2.50	B	0.80	229	GNM93		
SR20	...			B	0.071	225	GNM93		
ROXs 42C	...			B	0.157	135	GNM93	35.95	MWM89
Haro 1-4	4	−7.64	0.16	B	0.72	27	GNM93		
Haro 1-16	8	−5.86	0.41	S					
NTTS 160946-1851	1	−6.51	2.50	B	0.208	164	GNM93		
SR 4	7	−5.37	0.23	S					
NTTS 160815-1857	...			S				144	MWM89
Haro 1-14	2	−5.92	1.00	S					
NTTS 162218-2420	1	−3.57	2.50	B	0.236	156	GNM93		
V853 Oph	1	−7.99	2.50	B	0.399	96	GNM93		
NTTS 155913-2233	...			B	0.288	347	GNM93	2.42	MWM89
NTTS 160905-1859	...			S					
DoAr 24	...			S					
NTTS 155828-2232	1	−6.08	2.50	S					
NTTS 160827-1813	...			S					

GNM93 – Ghez et al. (1993).
GMPR97 – Ghez et al. (1997).
BA92 – Bouvier & Appenzeller (1992).
MWM89 – Mathieu et al. (1989).

Table 2. Individual radial velocity measurements for the sample stars. In each group of three columns, the first stands for the Heliocentric Julian Date, the second for the radial velocity (km s^{-1}) and the third for the error on the measurement (km s^{-1}).

SZCha			51008.4855	12.25	0.07				51675.7367	−88.65	0.01
50999.5212	15.87	0.26	51312.5100	11.21	0.09	Sz65			51683.8229	−88.59	0.01
51311.4771	16.57	0.27	51320.5818	10.96	0.09	51016.6278	−2.57	0.02	51685.7580	−88.56	0.01
51312.5812	15.73	0.33	51664.5336	10.91	0.08	51312.6827	−0.60	0.08			
51313.4786	16.98	0.32	51675.4891	9.79	0.09	51317.6335	−1.83	0.12	Th12		
51314.4911	14.84	0.23	51682.5055	8.89	0.17	51318.6623	−0.46	0.09	51006.5811	−1.79	0.06
51674.5219	15.72	0.41				51684.6787	1.34	0.05	51311.7419	−1.25	0.11
51684.6014	16.98	0.19	VZCha						51313.7612	−0.11	0.05
			51312.5512	18.76	0.37	Sz68			51664.7495	−0.64	0.06
LkHa332-20			51672.5627	17.18	0.08	51002.7169	−1.88	0.16	51672.6111	−1.84	0.04
51005.4876	15.07	0.17				51314.7663	−1.55	0.17	51674.8763	−0.78	0.03
51311.5087	15.77	0.16	CHX18N			51317.5607	−2.78	0.17	51682.7480	−0.41	0.04
51318.5592	15.97	0.18	51314.5357	15.71	0.10	51318.6879	−2.65	0.17	51685.8039	−0.06	0.02
51664.4857	14.50	0.15	51316.4792	15.82	0.08	51666.6401	−2.94	0.14			
			51316.4792	16.09	0.15	51671.6567	−2.49	0.10	RULup		
CSCha			51328.6360	15.91	0.20	51674.6068	−2.74	0.16	51003.7106	−1.92	0.06
51005.5356	14.68	0.05	51329.5472	14.65	0.20	51685.6580	−1.41	0.14	51316.6549	−1.77	0.09
51312.4721	15.48	0.04	51330.5715	14.86	0.20				51321.6779	−0.35	0.09
51319.5020	15.69	0.04				GWLup			51666.7141	−1.02	0.05
51665.5356	16.35	0.04	Sz41			51317.5954	−3.70	0.42	51672.6329	−2.48	0.05
51671.5806	17.50	0.05	51004.5582	14.74	0.17	51671.6932	−1.22	0.11	51674.7709	0.49	0.06
51683.5775	14.69	0.06	51314.5809	14.36	0.14				51685.6903	0.47	0.05
			51319.5944	14.99	0.14	GQLup					
CTCha			51665.5599	14.20	0.15	51003.6621	−3.57	0.02	RYLup		
51003.5429	14.84	0.09	51671.6314	14.17	0.12	51009.5413	−4.21	0.10	51005.6979	−3.27	0.20
51313.5198	15.69	0.14	51682.5483	13.70	0.15	51015.5502	−2.89	0.04	51316.6775	−2.30	0.18
51319.5278	15.53	0.08	51685.6123	13.25	0.12	51016.6840	−2.60	0.06	51321.6972	−1.00	0.16
51665.6120	15.84	0.05	51688.4979	14.07	0.12	51675.6512	−3.39	0.02	51666.6910	−2.95	0.12
51671.6060	15.06	0.06				51686.5603	−2.34	0.02	51672.6547	−1.04	0.09
51683.6204	13.97	0.10	LkHa332-21						51674.8392	−1.98	0.11
			51002.5202	15.99	0.09	Sz73			51685.7222	−1.66	0.09
LkHa332-17			51316.5093	15.40	0.10	51329.6124	−3.28	0.20			
51007.4927	14.61	0.24	51317.5292	16.74	0.13				He1125		
51010.4985	14.03	0.22	51318.6067	14.86	0.10	Sz77			51313.7933	0.14	0.08
51311.5353	14.08	0.32	51669.6369	15.70	0.10	51002.6696	−2.66	0.04	51667.6467	−0.49	0.12
51318.5831	14.32	0.16	51688.6404	16.05	0.12	51315.7035	−2.95	0.05	51672.7530	0.51	0.04
51666.5403	14.43	0.20	51315.5753	14.28	0.15	51321.6481	−2.34	0.03	51677.6260	−0.27	0.08
51675.5326	11.71	0.40				51664.6759	−2.45	0.05	51687.5914	0.40	0.03
51676.6352	14.18	0.15	HMAnon			51671.7367	−2.17	0.01	51688.6994	−1.11	0.05
51684.5652	14.02	0.16	51002.5751	13.91	0.01	51683.6667	−3.00	0.02			
			51314.6246	14.16	0.02				Sz85		
HM15			51319.6147	14.16	0.02	Sz78			51010.5495	−26.88	0.01
51305.5048	15.11	0.20	51664.6216	14.06	0.03	51004.6321	−6.28	0.01	51316.7225	−25.01	0.01
51306.4992	14.35	0.20	51665.5908	14.17	0.02	51315.7412	−6.50	0.01	51664.7856	−25.14	0.01
51328.5197	13.75	0.20	51682.5813	13.76	0.04	51320.6734	−6.50	0.02	51688.5774	−23.73	0.01
51329.4845	13.75	0.20				51665.7192	−6.45	0.01			
51670.5932	14.16	0.07	BFCha			51675.6938	−6.49	0.01	Sz126		
51676.5602	15.18	0.11	51311.6481	10.72	0.59	51683.7711	−6.40	0.01	51667.7374	−0.64	0.09
			51315.6202	13.00	0.51						
VWCha			51674.6630	11.84	0.28	Sz79			Sz128		
51311.6020	15.31	0.36	51686.5972	10.24	0.46	51005.5960	−88.70	0.01	51330.6723	−1.71	0.20
51669.6034	18.60	0.17				51316.5516	−88.57	0.01	51676.7624	0.10	0.08
			BMCha			51320.7071	−88.54	0.01			
CHXR32			51312.6360	10.30	0.66	51665.7481	−88.55	0.01	Sz130		

Table 2. continued.

51305.7634	0.19	0.20	51329.7304	0.00	0.20			
51306.7158	0.63	0.20	51330.7551	−2.35	0.20	NTTS155203-2338		
51667.7764	1.05	0.14	51687.8124	−2.80	0.12	51001.5647	−3.94	0.56
EXLup			Sz123			Haro1-4		
51319.6431	−3.08	0.09	51329.7722	−0.08	0.20	51012.6938	−7.44	0.08
51665.7993	0.18	0.05	51330.8001	−0.58	0.20	51318.7877	−7.57	0.03
						51669.8192	−7.78	0.02
Sz89			KnHa6			51686.8039	−7.75	0.02
51687.8560	−38.11	0.07	51002.7884	−1.04	0.22			
51688.6096	−37.00	0.10	51003.8835	−4.12	0.39	Haro1-16		
			51004.8611	−1.90	0.32	51007.7611	−6.53	0.13
HOLup						51315.8273	−5.54	0.10
51666.7437	−3.30	0.11	SCrA			51666.8937	−6.11	0.04
51668.8299	−2.42	0.09	51001.7323	2.90	0.26	51669.8584	−6.22	0.06
51677.7351	−3.24	0.18	51005.8098	−2.33	0.17	51675.8911	−5.85	0.10
			51005.8634	−1.25	0.21	51682.8760	−5.42	0.04
Sz90			51006.8744	0.26	0.22	51684.8484	−5.35	0.05
51305.7497	3.72	0.20	51007.8124	0.01	0.43	51686.7610	−5.88	0.03
51306.8243	−1.09	0.20	51008.7905	0.11	0.29			
51328.7800	0.57	0.20	51011.7296	−1.81	0.28	NTTS160946-1851		
51677.7781	−0.12	0.07				51006.7255	−6.51	0.91
51688.7434	−2.04	0.07	AS205					
			51314.8724	−11.36	0.42	SR4		
Sz91			51315.8745	−9.27	0.34	51006.6848	−5.20	0.05
51305.7942	−2.36	0.20	51316.7589	−9.70	0.18	51010.6432	−5.83	0.06
51306.8605	−1.85	0.20	51318.7470	−8.50	0.19	51316.8736	−5.20	0.03
51328.8253	−0.49	0.20	51675.8254	−10.40	0.35	51321.9044	−5.31	0.05
			51684.8056	−7.02	0.15	51671.8609	−5.24	0.02
Sz96						51676.8485	−5.53	0.02
51319.7184	−3.68	0.07	DoAr24E			51686.8483	−5.27	0.02
51666.8443	−3.28	0.05	51321.8087	−7.97	0.68			
51687.6728	−3.50	0.02				Haro1-14		
			V1121Oph			51013.6672	−6.62	0.09
HKLup			50999.7022	−9.23	0.07	51320.8453	−5.21	0.04
51319.7538	0.36	0.13	51313.9263	−8.88	0.05			
51666.7807	−2.08	0.06	51664.8213	−7.85	0.04	NTTS162218-2420		
51675.7820	−3.91	0.06	51671.8930	−8.50	0.03	51015.7181	−3.57	0.11
			51682.8192	−8.49	0.05			
Sz103			51686.6507	−8.76	0.02	V853Oph		
51330.8470	−1.32	0.20				51670.8562	−7.99	0.06
			SR9					
Sz105			51004.7793	−5.31	0.05	NTTS155828-2232		
51329.8110	1.70	0.20	51010.6934	−5.23	0.05	50999.6503	−6.08	0.04
			51313.9030	−8.10	0.06			
Sz110			51314.8318	−7.95	0.05			
51328.8577	0.27	0.20	51316.8402	−7.59	0.03			
51330.9100	−0.77	0.20	51318.8726	−5.44	0.03			
			51320.8135	−7.79	0.05			
Sz111			51321.7709	−9.50	0.05			
51672.8058	−1.35	0.03	51666.9406	−6.55	0.06			
			51669.8884	−7.20	0.05			
Sz117			51682.8425	−6.85	0.03			
51306.7508	−1.83	0.20	51686.7252	−7.83	0.03			

The radial-velocity error is estimated by using Eq. (9) of Baranne et al. (1996):

$$\sigma(V_r) = \frac{K}{D \times S/N} \times \frac{1 + 0.2w}{3}$$

where w is the FWHM of the observed CCF, D its depth and S/N is the signal-to-noise ratio in the CCF continuum. K is a constant which depends on the numerical mask used in the cross-correlation and on the spectral type of the observed

stars. For the stars in our sample, K is equal to 0.03 km s^{-1} (Queloz 1995). Typical values of S/N, D and w for our program stars give an internal error on the radial velocity measurement of about 0.2 km s^{-1}. It is worth mentioning that the expression for the error on V_r given above is valid for the case where the cross-corelation function is fairly symmetric around its minimum. However, phenomena like stellar activity or accreation can introduce deformities in the cross-correlation function (see BF Cha in Fig. 5, for instance). In these cases, the error on V_r as computed as above is underestimated. As more relistic estimate of the total radial velocity variability (error plus intrisic sources of variability), one can use the standard deviation of the V_r measurements, given Table 1. The $V \sin i$ derived for our sample are not given in this paper, instead they will be subject of a future work.

The number of observations, the mean radial velocity and the rms of the radial velocity measurements are given in Table 1. For stars with only one observation, we adopt $\sigma_{V_r} = 2.5$ km s^{-1}.

3. Results

3.1. Bias analysis

A delicate point in this kind of work is to know how many companions were missed because of the selection criteria of our sample and because of lack of sensitivity of our detector. As we have already pointed out, we took the same southern part of the sample as in GNM93 and the whole sample of GMPR97. Both studies were limited in apparent magnitude at K–band to $m_K = 8.5$. The mean apparent magnitude of the entire sample is $< m_K > \sim 7.7$. If we further assume a distance of $d = 150$ pc as the being the mean distance to the nearby star-forming-regions, we have a mean K-absolute magnitude $< M_K > \sim 1.8$. In order to transform the magnitude limit to mass limit we assume the mass–M_K relation given by Baraffe et al. (1998) at 2 Myr, that gives a mean primary mass of about $< M > = 1\ M_\odot$. Both GNM93 and GMPR97 are able to detect companions with magnitude differences up to $\Delta K \sim 3.0$. $\Delta m_k = \Delta M_K \sim 3.0$. Thus the lightest detectable companions have absolute K magnitude of about $M_{K,\min} = 4.8$. Again, using the mass–M_K relation given by Baraffe et al. at 2 Myr, we found that the lightest detectable secondaries have a mass of about 0.13 $M_\odot$. Thus, the two surveys presented in GNM93 and GMPB97 are complete down to mass ratio greater than about $q \gtrsim 0.1$–0.2.

In order to evaluate the completeness level of our survey we estimated the probability of detection of a binary system composed of a primary of one solar mass and a secondary of mass M_2, we proceed as described in Sect. 6.1 of Duquennoy & Mayor (1991). Briefly, to derive the probability of *detection* of a given point in the $(M_2, P_{\rm orb})$ space we generate $N_{\rm bin}$ artificial binaries with orbital elements T_0, ω, i randomly generated from a uniform distribution, while the eccentricity e follows the criteria:

1. for $P_{\rm orb} < 8$d, $e \equiv 0$ (Melo et al. 2001)
2. for $8 < P < 1000$d, e follows the eccentricity distribution obtained for the Hyades dwarfs (Mayor & Mermilliod 1984; Burki & Mayor 1985)
3. for $P > 1000$d, $f(e) = 2e$.

The artificial binaries are then "observed". This means that for each (real) star observed in the nights $n_1, n_2, ..., n_i$ during our survey, we have created $N_{\rm bin}$ artificial binaries. Then, the radial velocities of the artificial binaries are computed using the the actual dates $n_1, n_2, ..., n_i$. To these radial velocities, we add a random error generated from a normal distribution centered on zero and with a chosen rms value, $\sigma_{\rm err}$. If the rms of the radial velocities of the artificial binary (σ_{V_r}) is greater than $\sigma_{\rm err}$, the artificial binary star is declared as *detected*. The final detection probability at a point $(M_2, P_{\rm orb})$ is given by the number of detections divided by the number of stars in our survey times the number of artificial binaries, $N_{\rm bin}$. This method yields a sort of mean detection probability based on the observing dates of the whole sample, instead of using one single sampling function.

It is worth mentioning that for systems with $M_2 \sim 0.4\ M_\odot$ and with orbital periods greater than about one year (i.e. small values of radial velocity curve amplitude K_1), the probability surface strongly depends on $\sigma_{\rm err}$. Thus, if we underestimate our errors, many stars will be erroneously declared as detected. For active stars, like the T Tauri, the spread in the radial velocity measurements caused by their intrinsic variability, σ_i, is often higher than the internal error on individual measurements. By consequence, we must use σ_i instead of $\sigma_{\rm err}$ in the estimation of the missing companions. Guenther et al. (2001) observe that for some cases in their sample, stellar activity can induce radial velocity variations of about 4 km s^{-1}. We can take as an estimate for σ_i the standard deviation of the residues, σ(O–C), around the orbital solution for the known T Tauri binary systems. For the binaries listed in Mathieu et al. (1989), the σ(O–C) is between 1–3 km s^{-1}, the same value of σ(O–C) is observed for the binaries found by Covino et al. (2001). We ended up adopting a $\sigma_i = 2.5$ km s^{-1} which corresponds to the highest σ_{V_r} given in Table 1 calculated a posteriori based on our own radial velocity observations. In Fig. 2 we show the detection probability in the plane $M_2 - P_{\rm orb}$ computed as described above. The detection probability levels are, from black to white, less than 25% (black), 50%, 65%, 75%, and greater than 75% (white). We see for example that the probability of detecting a binary system of 1 month period composed of a primary of one solar mass stars and a secondary of 0.15 $M_\odot$ is about 60%. We see that down to a secondary of about 0.3 $M_\odot$, the detection probability within the orbital period range of 0–10 and 10–100 days are quite uniform (i.e., within each orbital period interval, the detection probability levels are essentially of only one color). Thus, we adopted a mean correction factor of 0.75 and 0.65 corresponding to the mean detection probability in the orbital period range of 0–10 days and of 10–100 days, respectively. On the other hand, for systems with orbital periods larger than 100 days, the detection probability is highly dependent on the secondary mass, ranging from 70% down to only 20%. Thus, due to this highly variable sensitivity, we prefer to disregard systems with orbital larger than 100 days in our binary frequency estimations.

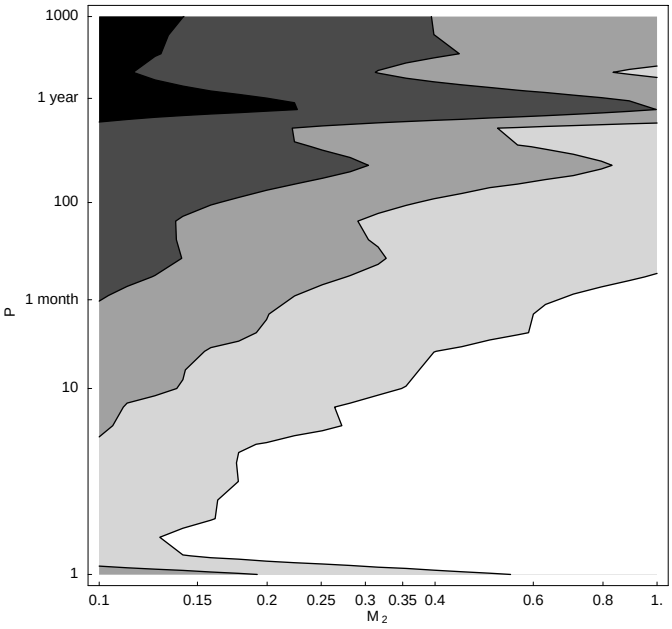

Fig. 2. Detection probability (lower than 25% (black), 50%, 65%, 75%, and greater than 75% (white)) as a function the secondary mass and orbital period. Period is given in days and secondary mass in solar masses.

Table 3. Number of stars, mean radial velocity, rms of the radial velocity for each SFR/cloud listed in Table 1.

Region	N	$< V_r >$ (km s^{-1})	$\sigma(V_r)$ (km s^{-1})
Cha I	13	15.0	1.7
Cha II	2	10.9	0.8
Lup I[1]	6	−2.4	0.9
Lup II	3	−2.7	3.2
Lup IV[2]	5	−0.6	1.0
Lup III[3]	12	−1.2	1.4
CrA	2	−1.3	1.5
Oph-Sco	13	−6.6	1.7

[1] Sz 79 was not taken into account.
[2] Sz 85 was not taken into account.
[3] Sz 89 was not taken into account.

3.2. SFR radial velocity distributions

The stars listed in Table 1 were separated accordingly to their region/cloud. The respective distributions of the radial velocity measurements are plotted in Fig. 3. The radial velocity distributions for Cha II, Lup II and CrA are only shown for sake of completeness. Since only two or three stars were observed in these regions/clouds, they add no significant information about the kinematics of these groups.

Let us now compare our radial velocity distributions with those available in the literature. The comparison of our observations with those from the literature is important since external data add another epoch to our radial velocity data which is important to trace long-period (of the order of several years) single-lined spectroscopic binaries. Dubath et al. (1996) published radial velocity data for a sample of 26 T Tauri stars supposed to be members of Cha I and Lup III. For ten stars in Cha I they also obtained the radial velocity of the gas in the line of sight towards each of these ten targets. Since they found no significant difference between the two radial velocity distributions, they concluded that these 10 stars are indeed bona fide T Tauri still bound to their parental cloud. Our mean radial velocity given in Table 3 for Cha I is of 14.9 ± 1.7 km s^{-1} which is in agreement to that of 14.8 ± 0.9 km s^{-1} found by Dubath et al. (1996) for these ten stars. In addition, the comparison of the individual measurements for 7 Cha I stars in common to the present work and that of Dubath et al. show a very good agreement, as we can seen looking at the filled circles in Fig. 4.

In the Lupus clouds, the agreement between our observations and those from the literature (Dubath et al. 1996; Wichimann et al. 1999) for the bona fide CTTS is also very good (filled squares in Fig. 4). In addition, we also observed two (Sz 85 and Sz 89) of the three high-velocity outlier stars found by Dubath et al. which are not shown in Fig. 3. Within the errors, our measurements are consistent with those of Dubath et al. that confirms their suggestion that these stars are possible members of the Carina arm and not merely long-period spectroscopic binaries, as suggested by the fact that their radial velocities are compatible with the heliocentric velocity of -36 km s^{-1} of a weak CO emission found by Murphy et al. (1986).

Finally, our radial velocity observations in Oph-Sco data are compared to those from Walter et al. (1994). As for Chameleon and Lupus, the agreement is also very good.

Looking at Fig. 4 we observe three deviant points, namely, VZ Cha, VW Cha and HK Lup. Let us analyze the possible causes of this deviant behavior. For VW Cha (Sz 24) Dubath et al. give a radial velocity of 21.2 km s^{-1} while we found 15.3 km s^{-1}. Dubath et al. also note that in the two additional radial velocity measurements obtained in a time interval of 20 months suggest that VW Cha has a constant velocity which is, however, very different from the radial velocity of the gas, they suggest that VW Cha could be a binary star. Indeed, one of our cross-correlation functions (see next section and Fig. 5) suggests the existence of three stars, one of them having a radial velocity consistent with the mean radial velocity of the association and other two stars which seem to wiggle as a SB2. Thus this system could be a triple, i.e., two visual components (which are indeed detected in GMPR97), with one of them being a spectroscopic binary. In the case of VZ Cha (Sz 31) Dubath et al. found a radial velocity of 38.2 km s^{-1} and a $V \sin i$ greater than 100 km s^{-1} whereas our 2 measurements give a mean radial velocity and mean $V \sin i$ of 17.97 and 8.50 km s^{-1}, respectively. In contrast to VW Cha, the cross-correlation of VZ Cha does not show any sign of a spectroscopic companion. If this star is a long-period single-lined spectroscopic binary we should expect then a constant $V \sin i$. Alternatively, we can suppose that this system is a very long period (i.e., very low amplitude) spectroscopic binary composed of two stars with mass not very different so the light of both of them contribute to the observed CCF, but, due to low amplitude, they never appear split in two peaks, instead we only see the changes in the width of CCF. The last one is HK Lup (Sz 98). The difference in

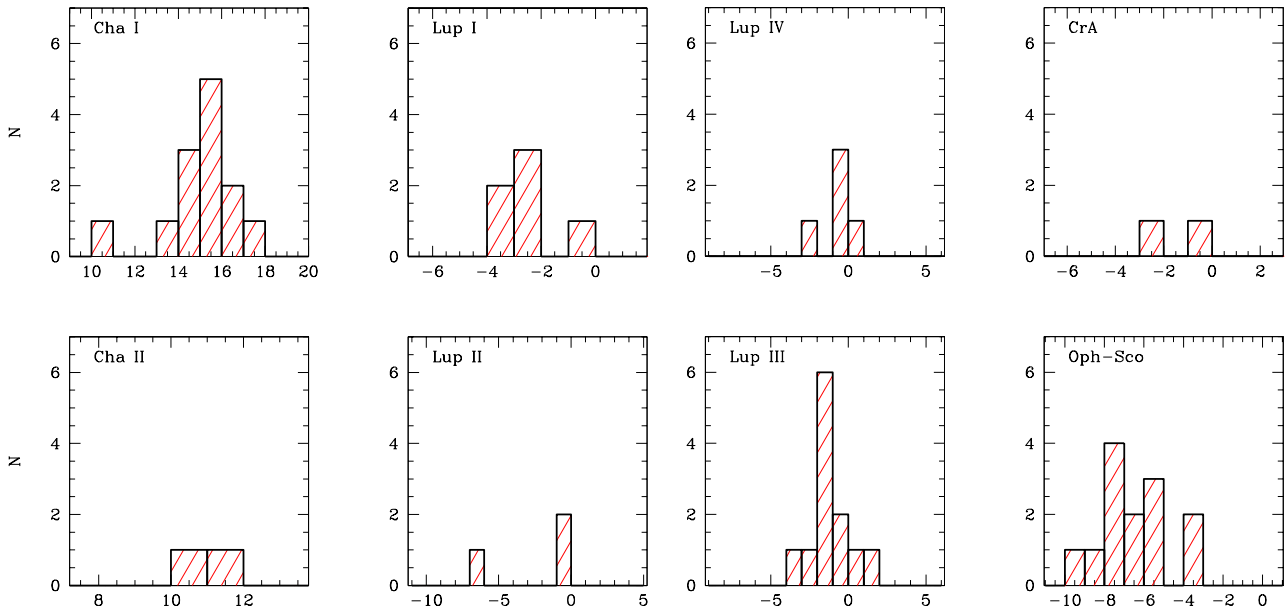

Fig. 3. Radial velocity distributions separated by SFR/cloud according to Table 1. Two (Sz 85 and Sz 89) of the three high-velocity outliers stars found by Dubath et al. (1996) in Lup III are not shown.

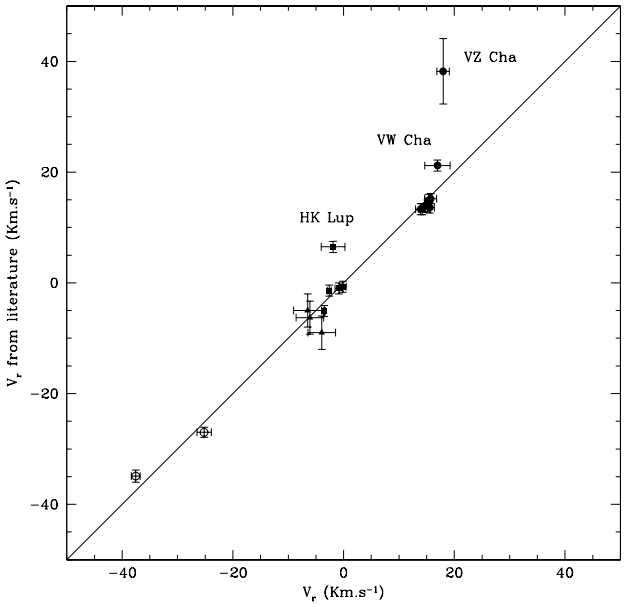

Fig. 4. Comparison between our radial velocities and those found in the literature. Filled circles, squares and triangles stand, respectively, for stars in Cha taken from Dubath et al. (1996), in Lup taken Dubath et al. (1996) and Wichmann et al. (1999) and in Oph taken from Walter et al. (1994). The two objects shown as open circles are the two possible member of the Carina-arm suggested by Dubath et al. (1996). The three deviant points (VZ Cha, VW Cha and HK Lup) are discussed in the text.

radial velocity between the measurements obtained by Dubath et al. and ours is of 8.4 km s^{-1} which is higher the uncertainties in both measurements. This suggests that this system might be a SB1. The information available about these three systems is clearly insufficient to allow us to correctly establish whether or not these three systems are spectroscopic binaries. Since we are not sure about the status of these three systems, we will disregard them in our spectroscopic binary frequency analysis of Sect. 3.

3.3. Spectroscopic binaries?

Our sample contains 4 spectroscopic binaries known a priori from the survey of Mathieu et al. (1989). In addition 4 stars showed at least once during our observations a double-lined cross-correlation function, namely:

- **VW Cha.** Line doubling was observed in the spectrum of 29th May 1999. Three stars are seen in the CCF of the 21st May 1999. In the other dates, the shape of the CCFs equally suggests the presence of at least one companion, thought less clearly than on the dates quoted above. The mean blend radial velocity is about 15.31 km s^{-1}.

- **CHX 18N.** Two stars are clearly seen in the CCF of the 14th May 1999 and less clearly in the CCF of the 19th May 1999. For the other observations, the radial velocity is stable at about 15.5 km s^{-1}.

- **BF Cha.** Despite of the noise in the observations, the CCFs of the 7 Jul. 1998, 12th May 1999, 14th May 1999 and 15th May 1999 suggest a binary system composed by a "slow" rotating star ($V \sin i \sim 17$ km s^{-1}) and a rapid rotating star ($V \sin i \sim 31$–36 km s^{-1}). The mean blend radial velocity is about 10–13 km s^{-1}. However, since the width of the cross-correlation function remains constant in the three observations, we suspect that the SB2 aspect which we are observing is due to variations in the line profiles caused by stellar rotation plus one or several spots on its surface (see e.g. Queloz 1999).

- **AS 205.** Line doubling was clearly observed only on the 13th May 1999. The mean blend radial velocity is of −9.0 km s^{-1}.

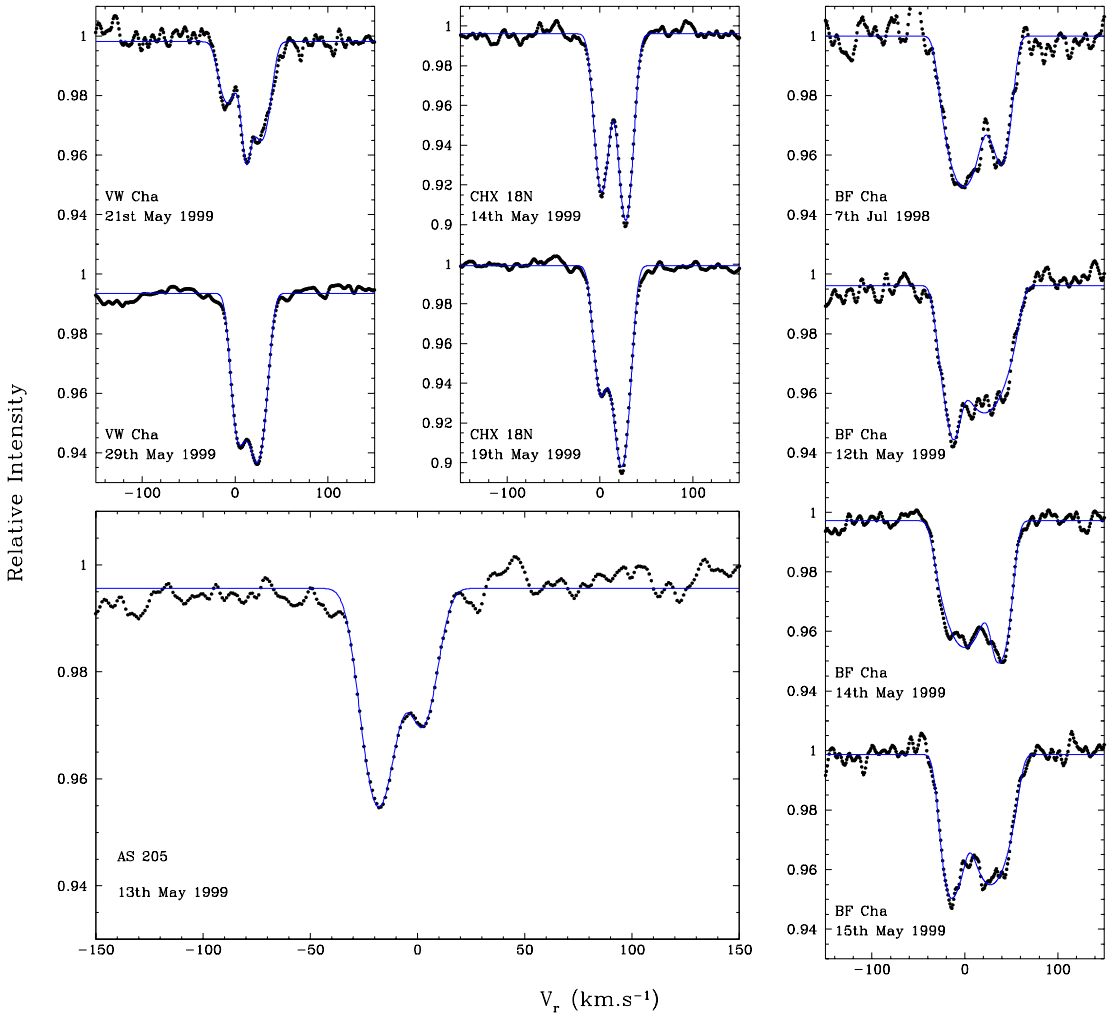

Fig. 5. The relative intensity of the CCF versus the radial velocity in km s^{-1} for the SB candidates identified during our survey. The name of the object and the date of the observation are indicated in the lower left corner of each CCF.

In Fig. 5 we show the double-lined CCFs for the objects referred above. The conclusion here is similar to that drawn in the last section, i.e., more observations are needed to establish whether or not these three systems are spectroscopic binaries. Meanwhile, these stars will be equally discarded in our analysis made in next section.

Concerning the other stars in our sample, they show standard deviation of the radial velocitiy measurements compatible with the standard deviation of the residuals around the orbital solution for the known T Tauri binary systems, i.e., 1–3 km s^{-1}. Therefore, these stars were classified as single stars ($\sigma(V_r) \leq$ 2.5 km s^{-1}). Nevertheless, a $\sigma(V_r) \lesssim 2.5$ km s^{-1} can be an artifact caused by the a bad sampling of the observing epochs, especially in the case of long period binaries. For instance, if ROX 43A (P_{orb} = 89.1d, e = 0.41 and K = 13.4 km s^{-1}, Mathieu et al. 1989) is observed at the same dates as VZCha, we would have a $\sigma(V_r) \sim 1.1$ km s^{-1}. While this effect can be statistically corrected for, as argued in Sect. 3.1, on an individual basis, the only way to confirm if such a system is a binary or not is with more observations.

3.4. Binary frequency

In Fig. 6 we present the spectroscopic companion star fraction (CSF) for the present Oph plus Cha/Lup/CrA combined sample (first two open bins with $0 \leq \log P_{orb} \leq 2$) along with the high-angular resolution (speckle, adaptive optics, direct imaging) CSF (last two open bins) from other studies. For each bin, the respective CSF of the G- and K-dwarfs of the solar neighborhood is shown as a hatched bin.

The spectroscopic CSF ($csf = \frac{B+2T+3Q}{S+B+T+Q}$) was computed by considering the 59 observed in our survey plus 6 other stars in Oph already observed for radial velocities (Mathieu et al. 1989; Mathieu 1992; Walter et al. 1994). As already mentioned above, we fail to find any new binaries besides those found Mathieu (1992, 1994). Within the interval $0 \leq \log P_{orb} \leq 1$ we count one triple system (NTTS155913–2233), thus the CSF in this interval of orbital period is of 0.03 (2/65). Applying the correction due to missed companions we have a corrected CSF of 0.04 (2/0.75/65). One binary (ROXs 43A) and one triple system (ROXs 42C) lie within the interval $1 \leq \log P_{orb} \leq 2$,

Table 4. The companion star fraction (CSF) of combined sample (Oph plus Cha/Lup/CrA) for different orbital separation domains as shown in Fig. 6. For the two visual binaries bins the final value of CSF for Cha/Lup/CrA+Oph sample was computed by simply averaging the corrected companion star fraction (CSF′) taken from Table 5 of GMPR97.

$\log P_{\rm orb}$	Angular sep.	csf	$csf_{\rm MS}$
0–1	0.″00016–0.″0008	0.04 ± 0.03	0.02 ± 0.02
1–2	0.″0008–0.″0035	0.07 ± 0.03	0.04 ± 0.03
4.5–6.0	0.″1–1.″2	0.28 ± 0.05	0.15 ± 0.05
6.0–7.6	1.″2–12.″0	0.24 ± 0.04	0.11 ± 0.04

the respective CSF is thus of 0.05 (3/65) and of 0.07 (3/.65/65) if a correction is applied.

For the domain of separation of 15-150 AU (i.e., 0.″1 up to 1.″2), we have taken the corrected companion star fractions (CSF′) computed in GMPR97 for Cha/Lup/CrA. For Oph, the CSF′ computed from the union of the results from GNM93 and Simon et al. (1995) was taken. The CSFs for the domain of separation of 150–1800 AU (i.e., 1.″2 up to 12.″0) for Cha/Lup/CrA and for Oph were taken respectively from GMPR97 and from Simon et al. (1995). All afore–mentioned values of CSF and CSF′ are compiled in Table 4. In each respective bin of separation the final value of CSF for Cha/Lup/CrA+Oph was computed by simply averaging the values taken from GMPR97.

The equivalent orbital period domain for each domain of separation was computed by assuming a distance of 150 pc to SFRs considered here, a total mass of 1 $M_{\odot}$ and that the semi major-axis a relates to the apparent separation ρ as $\overline{\log a} = \overline{\log \rho} + 0.1$ (Reipurth & Zinnecker 1993). For the same interval of orbital period, the respective CSF for the MS was estimated by integrating the analytical expression given by Duquennoy & Mayor (1991). Errors are calculated following the Poisson counting statistics, i.e., $\sigma \sim \sqrt{N}$, where N is the number of detections.

As we can see from Fig. 6 (and from Table 4), the PMS short period binary frequency within the errors is indistinguishable from that observed among the field G- and K-dwarfs. In contrast to the visual binary domain where the data are in abundance, little has been done to measure the PMS short period ($P_{\rm orb} < 100$ days) binary frequency. In fact, the only estimations up to now of the PMS short period binary frequency comes from Mathieu (1992, 1994). This lack of new results in this short range of period is likely due to the difficulty in measuring the spectroscopic binary frequency. While in the visual binaries domain, a few exposures per object generally taken in one observing run are enough to assess their binary nature, in the spectroscopic domain, unless we are dealing with a double-lined spectroscopic binary, several epochs are needed. Another important point is that the short period binary frequency is expected to be low (about 10%), thus large samples are needed to be able to unambiguously detect any possible excess between different populations.

The spectroscopic binary frequency and the errors computed in the present work are similar to those reported by Mathieu (1992, 1994). Indeed, the two samples in question have approximately the equal size (65 for this work against 55 in Mathieu 1992), consequently the statistical significance of the spectroscopic binary frequency estimations remains the same.

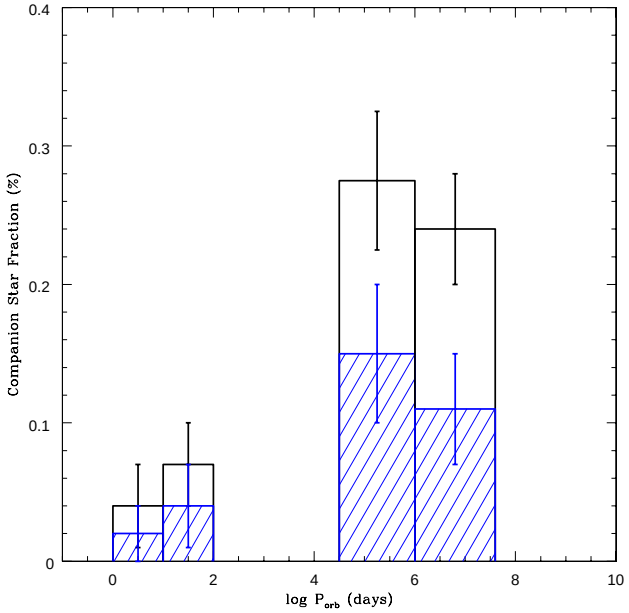

Fig. 6. The combined companion star fraction as a function of the orbital period for the sample of Cha/Lup/CrA+Oph. The first two open bins ($\log P_{\rm orb} \leq 2$) correspond to the spectroscopic binary frequency estimated in this paper, while the two right most ones come from a combination of the results of the resolution surveys presented in GNM93, GMPR97 and Simon et al. (1995), as explained in the text. The equivalent orbital period domain for each domain of separation was computed by assuming a total mass of 1 $M_{\odot}$ and that the semi major-axis a relates to the apparent separation ρ as $\overline{\log a} = \overline{\log \rho} + 0.1$ (Reipurth & Zinnecker 1993). For the same interval of orbital period, the respective CSF for the MS, which is shown as hatched bins, was estimated by integration of the the analytical expression given by Duquennoy & Mayor (1991).

While the combined spectroscopic binary frequency for Cha/Lup/CrA+Oph are indistinguishable from that observed for the field solar-type stars, the spectroscopic binary frequency for Oph-Sco alone is very high. In fact all confirmed binaries in our sample come from Oph-Sco which yields an uncorrected multiple star fraction (MSF, which is defined as $msf = \frac{B+T+Q}{S+B+T+Q}$) of 16% ± 9% (3/19) against 9.7% ± 2% (16/164) for the MS field stars. In contrast to Oph-Sco, no spectroscopic binary was found when only the stars in Cha/Lup/CrA were considered. Interestingly enough, Mathieu (1992) also found evidence for an excess of a factor 2.5 of binaries in Oph (given the MS frequency, they should find 2 short-period binaries in a sample of 24 stars, instead they found 5) while in Taurus, the number of short-period binaries expected in a sample containing 62 stars was 4–5, instead only one binary was found, similarly to what is observed here in Cha/Lup/CrA.

4. Discussion

The results of several high-angular resolution studies devoted to the measurement of the visual binary frequency among the PMS stars in different SFRs and young clusters suggest that the excess of binaries initially observed among the PMS populations is not universal. Duchêne (1999) summarizes and reanalyzes the results of these high-angular resolution surveys in order to consistently compare their results. If, on one side, Duchêne's analysis does not allow one to assess differences in the overall binary frequency and/or in the shape of the orbital period distribution, it allows, on the other hand, to compare the results of the different studies within a restricted range of separation. One conclusion which can be drawn from such an analysis is that low-density SFR, most notably Taurus, present a binary frequency higher by a factor 2 than that of the field solar-type stars, denser SFRs like Orion and young clusters exhibit similar fractions of low-mass visual binaries (for references on individual surveys, see Duchêne 1999; Patience & Duchêne 2001; Mathieu 1996)

There are currently two plausible alternatives to link the stellar formation and the differences observed in the visual CSFs (see Bouvier et al. 2001; Ghez 2001; Larson 2001; Clarke 2001 for recent reviews on the subject). The first one suggests that the differences in the observed CSFs are signatures that the outcome of stellar formation depends on the physical properties of the medium such as temperature, shape of parental cloud, magnetic field, etc. (e.g., Durisen & Sterzik 1994; Boss 2001). In the second alternative, the binary frequency resulting from the stellar formation process would be nearly constant, dynamically evolving afterwards through collisions (e.g., Kuopra 1995).

In this discussion the short period binary systems have a role to play. Kroupa (1998) studies the imprints, such as stellar velocity, system mass and binary proportion, left by the dynamical interactions occurred in aggregates of different concentrations. He shows that binary systems with an orbital period shorter than 1000 days are not ionized by dynamical interactions since their binding energies are greater than the mean kinetic energy of the population. On the other hand, in binary-binary or three body encounters these binaries are very likely to gain binding energy which means that, by conservation of energy, the pertuber body will gain kinetic energy and, depending on its mass, it can even escape from the potential well of the aggregate. The binary system, in turn, experiences a recoil which may be sufficient to also expel it from the aggregate (Kroupa 1998, see also Reipurth 2000 and Reipurth & Clarke 2001 for a review on the basic properties of three-body interactions and its role in the brown dwarf formation). Thus *the short-period binaries observed in a given cluster or association, are very likely to be the result of the formation process itself.* Of course that this is not exactly true for systems with $P_{\rm orb} \lesssim 10$ days, since they are very likely to undergo tidal interactions, mass transfers, etc. Also, the mass of the components is probably changing since both components will continue to accrete from its envelope, unless the systems has been ejected from this later.

How do close binaries form? The answer is not presently known. In a recent review, Bonnell (2001, see also Bodenheimer et al. 2000) identifies two major ways to form short-period binaries, namely, fragmentation and the dynamical migration of an initial wider pair. In the first mechanism, the binaries are already formed as a close pair, probably by fragmentation at the end of the second collapse phase, since at this point the Jeans radius is of the order of $\lesssim$1 AU. Once formed, the two fragments need to accrete the majority of their final stellar mass. The problem with this scenario is that fragmentation in unlikely to occur at this point (e.g. Boss 1989). In the second scenario, wide binaries are formed having a circumbinary disk which produces a torque in the system. This torque will transfer angular momentum from the binary to the disk. As a consequence, the disk will tend to expand and the central binary to became more hardly bound (i.e., the components get closer). In a recent paper, Tokovinin & Smekhov (2002) report the results of a long-term radial velocity campaign aimed at looking for spectroscopic sub-systems around a sample of visual multiples of spectral type F5-M. Their results show that the frequency of spectroscopic sub-systems in close visual binaries is similar to the field (11%–18%). However, spectroscopic sub-systems are more frequent among wide visual binaries (20%) and among the wide tertiary components of the known visual or spectroscopic binaries (30%). In addition, the majority of these sub-systems have an orbital period less than 7 days (Tokovinin & Smekhov 2002; Tokovinin 1997). They suggest that these (real) excess of short-period spectroscopic sub-systems is an imprint left by the formation mechanism. Such mechanism is similar to proposed above (i.e., the spectroscopic binary transfers orbital momentum to the disk which expands), but in the case of a triple system, the orbital angular momentum is transfered from the inner orbit to the external orbit, as a consequence the orbit of the spectroscopic sub-systems shrinks while the tertiary becomes wider. Eventually the two componets will be closer enough so tidal effects become important and acctually dictates the further orbital evolution (e.g. Kiseleva et al. 1998).

In fact, looking at our Table 1 we observe the same excess of close spectroscopic binaries among triple system as reported by Tokovinin & Smekhov (2002). Counting all the SBs (the bona-fide one plus the candidates) for stars without and with one or more visual companion, we see that 1.8%–5.7% of the SBs have no visual companion while 9%–14% do have one or more visual companion (i.e., they are spectroscopic sub-systems). Alternatively, if we consider only Sco-Oph stars and the confirmed SBs, we see that the percentage of SB without visual companion is of 8.3%, while the frequency of SBs having one or more visual companion is of 25%. The results shown above are of course affected by the low counts. Nevertheless, the data clearly show a trend in the direction of the Tokovinin & Smekhov's suggestion, namely, the frequency of spectroscopic binaries is higher among higher order (mainly triple) systems.

Another feature in the data is the excess (lack) of short period binary found in Oph (Taurus and Lup/Cha/CrA). Are the trends real? Undoubtedly, the small size of both samples mars any attempt of drawing a robust answer to these questions. In spite of that, in some cases one single exposure could have been enough to *detect* the binary nature of the object according to the following argument. Since the surface of the cross-correlation peaks are roughly proportional to the stellar luminosity

(see e.g. Pasquini et al. 1991), we can arbitrary state that the secondary peak would be seen in the cross-correlation if it is larger than 10% the surface of the primary. This can be translated into a magnitude difference of 2.5 in the CORALIE and/or FEROS bandpass. Thus considering that the primary is a star of one solar mass we find that such difference in V magnitude corresponds to a secondary of ∼0.5 $M_{\odot}$. Thus our conclusion is that there is a probability that systems with $P_{\rm orb} \lesssim 100$ days and $q \gtrsim 0.5$ can be at least detected or classified as SB2 candidate on the basis of a single exposure. This suggests that the lack of SBs observed in Taurus and Lup/Cha/CrA may be real. On the other hand, if additional observations prove that the 4 ambiguous (Sects. 3.2 and 3.3) cases in Cha/Lup/CrA are indeed spectroscopic binaries, then the MSF for Lup/Cha/CrA would be about 7% ± 3 what is not far from that found for the solar-type field stars. Thus more observations are clearly needed to resolve the issue whether or not there is a lack of spectroscopic binaries in Cha/Lup/CrA. If, however, further studies of short-period binary frequency based in larger samples confirm this difference between Oph in one side and Taurus and Cha/Lup/CrA at the other, this may suggest that the conditions favorable to the fragmentation at the end of the second collapse may have been found in some clouds, like Oph, and not in others like Taurus.

Finally, we would like to draw attention to a last interesting point concerning the shape of binary frequency distribution as a function of the orbital period. Kroupa & Burkert (2001) present the results numerical simulations performed in order to tackle the question of whether an initial narrow distribution of orbital periods can be broaden via dynamical interactions. They find that, even in extremely compact clusters, dynamical interactions cannot widen the period distribution sufficiently to explain the range of orbital period observed in clusters and associations of different ages. They conclude by suggesting that the wide range of orbital periods is a result of cloud fragmentation and subsequent magneto-hydrodynamical process. In the same direction, Bodenheimer & Burkert (2001) recognize that the actual fragmentation simulations do not explain the formation of close binaries. However, due to the smoothness of the transition in the binary frequency distribution between the close binary and the wide binary regime, they find it unlikely that there exists a second mechanism other than fragmentation which would account for the close binaries. Nevertheless, we could speculate that binary frequency distribution which we observe for the field solar-type stars results from a superpositions of different modes of stellar formation. If, on the other hand, the binary frequency distribution for a given association or SFR presents a real gap at $\log P_{\rm orb} \sim 3$–4, it could indicate that close binaries are formed differently from wide binaries. Again, the answer to this question lies on the determination of the whole binary frequency distribution as a function of orbital period for young populations which at the moment is not possible to determine, since radial velocity surveys are not of long enough duration to find objects with thousands of days of period and high-angular resolution techniques are not able to detect companions below about 10 000 days of period.

5. Summary

In this paper we have presented the results of a three-years high-resolution spectroscopic campaign conducted with the aim of estimating the spectroscopic binary frequency for a sample of T Tauri stars already surveyed for visual companions using high-angular resolution techniques by Ghez et al. (1993) and by Ghez et al. (1997).

- For a few stars in our sample we could obtain radial velocity measurements from the literature. The agreement between our values and the latter is very good. Three deviant cases were found for which the existence of a spectroscopic companion is not ruled out by the present data. The same conclusion holds for the objects presented in Sect. 3.3. for which a double-lined cross-correlation function was seen at least once during our campaign.
- Excepting these doubtful cases and the 4 binaries known a priori from Mathieu et al. (1989), no star presented a $\sigma_{V_{\rm r}}$ greater than 2.5 km s^{-1}. The radial velocity data presented in Table 1 can be useful for future radial velocity surveys as they can inform about the variability of stars observed in this work.
- The PMS short-period companion star fraction (CSF) found in our survey is indistinguishable from that found Duquennoy & Mayor (1991) for the field solar-type stars, confirming the previous results form Mathieu (1992) and Mathieu (1994).
- The data suggest that the spectroscopic binary frequency for Oph-Sco alone could be higher than that of the field solar-type stars by a factor of about 2. However, the paucity of the sample prevents us from drawing any robust conclusion about a possible excess. The questions as to whether or not such excess is real and whether or not there is a difference in the short-period binary frequency for different SFRs remain open.
- The spectroscopic binary frequency among the components of visual multiple systems is higher than in the stars without any visual companion, being between 1.8%–5.7% and 9%–14% respectively. If only the Sco-Oph and the confirmed SBs are considered, these numbers are highly increased. In this case the rate of SB without visual companion is of 8.3% while the frequency of SBs having one or more visual companion is of 25%. This trend is similar to the results reported by Tokovinin & Smekhov (2002) for solar-type stars and it is probably a signature of the formation mechanism of the spectroscopic binaries.

In order to provide a solid (in the statistical sense) answer to these questions, a survey must to be performed with a sample containing several hundreds of stars, such a program is well suited to multi-object spectrograph like GIRAFFE.

Acknowledgements. CHFM is very obliged to Prof. Michel Mayor whose support was fundamental to the realization of this work, either through the allocation several nights in the Swiss Euler Telescope or through his always enlightening comments. Jean-Claude Mermilliod, Bo Reipurth, Michael Sterzik, Juan Alcalà, Elvira Covino and Nuno Santos are also warmly acknowledged for helpful discussions. This work was partially supported by CNPQ proc. 200614/96-7 (NV).

This research has made use of the Simbad database, operated at CDS, Strasbourg, France. Finally, we wish to thank the referee for his/her helpful comments.

References

Baraffe, I., Chabrier, G., Allard, F., & Hauschildt, P. H. 1998, A&A 337, 403
Baranne, A., Queloz, D., Mayor, M., et al. 1996, A&AS 119, 373
Bodenheimer, P., Burkert, A., Klein, R. I., & Boss, A.P. 2000, in Protostars and Planets IV, ed. V. Mannings, A. P. Boss, & S. S. Russell (Tucson: University of Arizona Press), 675
Bodenheimer, P., & Burkert, A. 2001, in Formation of binary stars, ed. H. Zinnecker, & R. D. Mathieu, IAU Symp., 200, 13
Bonnell, I. 2001, IAU Symp. 200, ed. H. Zinnecker & R. D. Mathieu, 23
Boss, A. P. 1989, ApJ, 346, 336
Boss, A. 2001, IAU Symp. 200, ed. H. Zinnecker & R. D. Mathieu, 371
Bouvier, J., & Appenzeller, I. 1992, A&AS, 92, 481
Bouvier, J., Rigaut, F., & Nadeau, D. 1997, A&A, 323, 139
Bouvier, J., Duchêne, G., Mermilliod, J.-C., & Simon, T. 2001, A&A, 375, 989
Brandner, W., & Köhler, R. 1998, ApJ, 499, L79
Burki, G., Mayor, M. 1985, in Instrumetation and Research Programmes for Small Telescopes, ed. J. B. Hearnshaw, P. L. Cottrell (Dordrecht: Reidel), 385
Clarke, C. 2001, in Formation of binary stars, ed. H. Zinnecker, & R. D. Mathieu, IAU Symp., 200, 346
Covino, E., Melo, C. H. F., Alcalá, J. M., et al. 2001, A&A, 375, 130
Dubath, P., Reipurth, B., & Mayor, M. 1996, A&A, 308, 107
Duchêne, G. 1999, A&A, 341, 547
Duchêne, G., Bouvier, J., & Simon, T. 1999, A&A, 343, 831
Durisen, R. H., & Sterzik, M. F. 1994, A&A, 286, 84
Duquennoy, A., & Mayor, M. 1991, A&A, 248, 485
Ghez, A. M., McCarthy, D. W., Patience, J. L., & Beck, T. L. 1997, ApJ, 481, 378
Ghez, A. M., Neugebauer, G., & Matthews, K. 1993, AJ, 106, 2005
Ghez, A. M. 2001, IAU Symp. 200, ed. H. Zinnecker, & R. D. Mathieu, 210
Gray, D. 1976, The Observation and Analysis of Stellar Photosphere (Wiley & Sons, Inc.)
Guenther, E. W., Neuhäuser, R., Joergens, V., et al. 2001, 11th Cool stars, stellar systems and the Sun, CD-515
Kaufer, A., Stahl, O., Tubbesing, S., et al. 1999, The ESO Messenger 95, 8
Kiseleva, L. G., Eggleton, P. P., & Mikkola, S. 1998, MNRAS, 300, 292
Kroupa, P. 1995, MNRAS, 277, 1522
Kroupa, P. 1998, MNRAS, 298, 231
Kroupa, P., & Burkert, A. 2001, ApJ, 555, 945
Larson R. 2001, in Formation of binary stars, ed. H. Zinnecker, & R. D. Mathieu, IAU Symp., 200, 93
Leinert, C., Zinnecker, H., Weitzel, N., et al. 1993, A&A, 278, 129
Mathieu, H. D. 1992, in Complementary Approaches to Double and Multiple Star Research, ed. H. A. McAlister, & W. I. Hartkopf, IAU Colloq., 135, 30
Mathieu, R. D. 1994, ARA&A, 32, 465
Mathieu, R. D. 1996, ASP Conf. Ser. 90, ed. E. F. Milone, & J.-C. Mermilliod, 231
Mathieu, R. D., Walter, F. M., & Myers, P. C. 1989, AJ, 98, 987
Mayor, M., & Mermilliod. J.-C. 1984, Observational tests of the Stellar Evolution Theory, ed. A. Maeder, & A. Renzini (Dordrecht: Reidel), 411
Melo, C. H. F., & Covino, E., & Alcalá, J. M., & Torres G. 2001, A&A, 378, 898
Murphy, D. C., Cohen, R., & May J. 1986, A&A, 167, 234
Pasquini, L., Cutispoto, G., Gratton, R., & Mayor, M. 1991, A&A, 248, 72
Patience, J., & Duchêne, G. 2001, in The Formation of Binary Stars, ed. H., Zinnecker, & R. D., Mathieu, IAU Symp., 200, 181
Patience, J., Ghez, A. M., Reid, I. N., Weinberger, A. J., & Matthews, K. 1998, AJ, 115, 1972
Queloz, D., Ph.D. Thesis, Geneva Observatory, 1995
Queloz, D., Allain, S., Mermilliod, J.-C., Bouvier, J., & Mayor, M. 1998, A&A, 335, 183
Queloz, D. 1999, in Planets Outside The Solar System, ed. J.-M., Mariotti, & D., Alloin, NATO Science Ser. C , 532, 229
Queloz, D., Mayor, M., Naef, D., et al. 2000, in VLT Opening Symposium, From extrasolar planets to brown dwarfs, ESO Astrophys. Symp., ed. J. Bergeron, & A. Renzini, 548
Press, W. H., Teukolsky, S. A., Vetterling, W. T., & Flannery, B. P. 1992, Numerical Recipes in Fortran 2nd ed. (Cambridge University Press)
Reipurth, B. 2000, AJ, 120, 3177
Reipurth, B., & Clarke, C. 2001, AJ, 122, 432
Reipurth, B., & Zinnecker, H. 1993, A&A, 278, 81
Richichi, A., Leinert, C., Jameson, R., & Zinnecker, H. 1994, A&A, 287, 145
Simon, M., Ghez, A. M., Leinert, C., et al. 1995, ApJ, 443, 625
Tokovinin, A. A. 1997, A&AS, 124, 75
Tokovinin, A. A., & Smekhov, M. G. 2002, A&A, 382, 118
Walter, F. M., Vrba, F. J., Mathieu, R. D., Brown, A., & Myers, P. C. 1994, AJ, 107, 692
Wichmann, R., Covino, E., Alcalá, J. M., et al. 1999, MNRAS, 307, 909
Zahn, J.-P. 1977, A&A, 57, 383